

Measurements of ocean derived aerosol off the coast of California

T. S. Bates,¹ P. K. Quinn,¹ A. A. Frossard,² L. M. Russell,² J. Hakala,³ T. Petäjä,³ M. Kulmala,³ D. S. Covert,⁴ C. D. Cappa,⁵ S.-M. Li,⁶ K. L. Hayden,⁶ I. Nuaaman,^{6,7} R. McLaren,⁷ P. Massoli,⁸ M. R. Canagaratna,⁸ T. B. Onasch,⁸ D. Sueper,⁸ D. R. Worsnop,⁸ and W. C. Keene⁹

Received 7 February 2012; revised 17 May 2012; accepted 20 May 2012; published 29 June 2012.

[1] Reliable characterization of particles freshly emitted from the ocean surface requires a sampling method that is able to isolate those particles and prevent them from interacting with ambient gases and particles. Here we report measurements of particles directly emitted from the ocean using a newly developed in situ particle generator (Sea Sweep). The Sea Sweep was deployed alongside R/V *Atlantis* off the coast of California during May of 2010. Bubbles were generated 0.75 m below the ocean surface with stainless steel frits and swept into a hood/vacuum hose to feed a suite of aerosol instrumentation on board the ship. The number size distribution of the directly emitted, nascent particles had a dominant mode at 55–60 nm (dry diameter) and secondary modes at 30–40 nm and 200–300 nm. The nascent aerosol was not volatile at 230°C and was not enriched in SO_4^- , Ca^{++} , K^+ , or Mg^{++} above that found in surface seawater. The organic component of the nascent aerosol (7% of the dry submicrometer mass) volatilized at a temperature between 230 and 600°C. The submicrometer organic aerosol characterized by mass spectrometry was dominated by non-oxygenated hydrocarbons. The nascent aerosol at 50, 100, and 145 nm dry diameter behaved hygroscopically like an internal mixture of sea salt with a small organic component. The CCN/CN activation ratio for 60 nm Sea Sweep particles was near 1 for all supersaturations of 0.3 and higher indicating that all of the particles took up water and grew to cloud drop size. The nascent organic aerosol mass fraction did not increase in regions of higher surface seawater chlorophyll but did show a positive correlation with seawater dimethylsulfide (DMS).

Citation: Bates, T. S., et al. (2012), Measurements of ocean derived aerosol off the coast of California, *J. Geophys. Res.*, 117, D00V15, doi:10.1029/2012JD017588.

1. Introduction

[2] Breaking waves on the ocean surface entrain air into the upper ocean. When the air bubbles rise to the surface they

inject seawater drops (sea spray) into the atmosphere. Sea spray, as used here, includes both the inorganic and organic components found in surface seawater. Sea salt includes only the inorganic salts. Sea spray particles in the atmosphere scatter solar radiation, act as cloud condensation nuclei (CCN), and affect atmospheric chemistry through multiphase reactions. Over the remote oceans, coarse-mode (0.5–10 μm dry aerodynamic diameter) sea-salt particles dominate aerosol light scattering [Quinn *et al.*, 1998]. Particles in this size range scatter light efficiently but contribute little to the total particle number concentration. Sea spray particles in the 0.01–0.2 μm dry diameter size range over the remote oceans can be the dominant source of CCN [Cipriano *et al.*, 1987; O'Dowd and Smith, 1993; Leck and Bigg, 2005; Clarke *et al.*, 2006]. The chemical composition of these particles is difficult to measure with mass-based methods because there is little mass in this size range. Direct impactor measurements of the size-resolved chemical composition of marine aerosol produced artificially by bubbling air throughflowing N. Atlantic seawater indicate that the dry mass of particles with diameters less than 100 nm is dominated by organic compounds [e.g., Keene *et al.*, 2007; Facchini *et al.*, 2008].

¹Pacific Marine Environmental Laboratory, NOAA, Seattle, Washington, USA.

²Scripps Institution of Oceanography, University of California, San Diego, California, USA.

³Department of Physics, University of Helsinki, Helsinki, Finland.

⁴Department of Atmospheric Sciences, University of Washington, Seattle, Washington, USA.

⁵Department of Civil and Environmental Engineering, University of California, Davis, California, USA.

⁶Air Quality Research Division, Science and Technology Branch, Environment Canada, Downsview, Ontario, Canada.

⁷Center for Atmospheric Chemistry, York University, Toronto, Ontario, Canada.

⁸Aerodyne Research, Billerica, Massachusetts, USA.

⁹Climate Change Research Center, University of Virginia, Charlottesville, Virginia, USA.

Corresponding author: T. S. Bates, Pacific Marine Environmental Laboratory, NOAA, 7600 Sand Point Way NE, Seattle, WA 98115, USA. (tim.bates@noaa.gov)

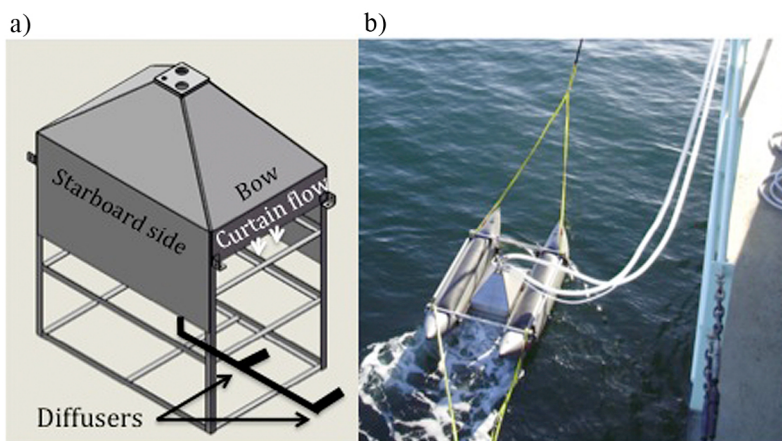


Figure 1. (a) Sea Sweep frame and coverings. (b) Sea Sweep deployed off the port bow of the R/V *Atlantis*.

Transmission electron microscope (TEM) photographs in the high Arctic and the tropics suggest that most of the smaller particles (15–70 nm) are microcolloidal aggregates [Leck and Bigg, 2005; Bigg and Leck, 2008]. In contrast, indirect methods including volatility and hygroscopicity measurements suggest that most of the sea spray in this size range is sea salt [O’Dowd and Smith, 1993; Clarke *et al.*, 2006]. Knowledge of the composition and source function of these particles is critical for parameterizing effects of aerosols on cloud properties and aerosol-cloud interactions in climate models.

[3] Atmospheric aerosols over the ocean include primary particles directly emitted from the ocean and associated reaction products, particles produced in the atmosphere via nucleation and growth pathways, and particles mixed into the marine boundary layer (MBL) from the free troposphere. It is difficult to distinguish between these three sources based on measurements of ambient aerosol. Characterization of particles freshly emitted from the ocean surface requires a sampling method that is able to isolate those particles and prevent them from interacting with ambient gases and particles. We describe here a newly developed method (Sea Sweep) for generating and sampling nascent sea spray particles to determine their chemical composition and microphysical- and cloud-nucleating properties.

2. Methods

2.1. Sea Sweep

[4] The Sea Sweep consists of a frame of stainless steel (ss) flatbar 0.61 m wide, 0.91 m long, and 0.91 m high (Figure 1). The upper 0.15 m (bow and stern) and 0.46 m (port and starboard sides) of the frame are covered with ss sheet metal. The top is enclosed with ss sheet metal hood in a cone shape extending 0.3 m above the frame. The Sea Sweep frame is supported by two inflatable pontoon floats (1000 Denier Reinforced) 3 m long attached to aluminum tubing. The frame was adjusted in the pontoons so that the opening at the bow and stern was 1.0 cm above the water under calm conditions.

[5] Three hoses are attached to the Sea Sweep cone top. One hose (1.3 cm ID Pliovic™ reinforced (braided))

provides compressed air at a flow of 50 L min^{-1} to two ss diffusion stones (2 μm porosity, 2.54 cm diameter, 24 cm long). The diffusion stones are horizontally mounted on the bottom of the Sea Sweep frame 0.75 m below the sea surface. A second hose (5.1 cm ID NutriFLEX Pliovic™) provides a laminar flow air curtain directed downward at the bow and stern ends of the frame. A blower is used to produce a flow of $2 \text{ m}^3 \text{ min}^{-1}$ of particle-free air (charcoal and hepa filtered) to form this curtain. The curtain and sidewalls prevent ambient air from entering the Sea Sweep. The curtain provides an outward flow of about $1 \text{ m}^3 \text{ min}^{-1}$ (1 m sec^{-1} face velocity) and an equal dilution flow to the bubbled air in the enclosed space under the hood. The third hose (5.1 cm ID NutriFLEX Pliovic™) brings $1 \text{ m}^3 \text{ min}^{-1}$ of Sea Sweep “sample” air to the PMEL aerosol sampling mast 18 m above the sea surface. This is the same mast and flow rate used during ambient air sampling. The transmission efficiency of the PMEL sampling mast for particles with aerodynamic diameters less than $6.5 \mu\text{m}$ (the largest size tested) is greater than 95% [Bates *et al.*, 2002]. To check for particle losses, simultaneous measurements of the aerosol number size distribution resulting from bubbled seawater were made at the top of the Sea Sweep cone and at the base of the sampling mast with two Aerodynamic Particle Sizers (APS). These measurements showed no measurable loss of particles in either the hose or the mast.

[6] The Sea Sweep was deployed off the port bow of the R/V *Atlantis* during CalNEX. The ship was positioned with the wind off the starboard bow and steamed slowly (0.2 m sec^{-1}) forward during sampling to ensure a continual renewal of ocean surface water. The forward motion was relative to the current. During some deployments, the ship steamed slowly backward to keep the water flow under Sea Sweep at 0.2 m sec^{-1} . The ship motion was adjusted visually to keep some bubbles trailing behind Sea Sweep while most of the bubbles were captured in the hood. The ship blocked the true wind.

2.2. Aerosol Sampling

[7] The bottom 1.5 m of the mast and the humidity controlled chamber at the base of the mast containing the impactors, nephelometers and sizing instruments were heated

or cooled to establish a stable reference relative humidity (RH) for the sample air of $\approx 60\%$. A stable reference RH allows for constant instrumental size segregation and results in chemical, physical, and optical measurements that are directly comparable. A reference RH of 60% was chosen because it is above the crystallization humidity of most aerosol components and component mixtures [Carrico *et al.*, 2003]. An aerosol mass spectrometer (AMS) was located outside the humidity controlled chamber, however the sampling line was maintained at 60% RH. A thermo-denuder twin scanning mobility particle sizing (SMPS) system, an hygroscopic tandem differential mobility particle sizing (DMPS) system, a Photoacoustic Absorption Spectrometer (PAS), a Cavity Ring-Down Spectrometer (CRDS), and a Single Particle Soot Photometer (SP2) were also located outside the humidity-controlled chamber. These sample lines were dried with nafion driers to an RH of less than 20% before sampling.

[8] Twenty-one 1.6 cm outer diameter stainless steel tubes extended into the heated portion of the mast. These were connected to the aerosol instrumentation and impactors with conductive silicon tubing to prevent electrostatic loss of particles or stainless steel tubing for the lines to the impactors used for collection of carbonaceous aerosol and the AMS.

2.3. Sea Sweep Aerosol Chemical Composition

[9] Samples using one and two-stage multijet cascade impactors [Berner *et al.*, 1979] were used to determine sub- and supermicrometer concentrations of inorganic ions and organic and elemental carbon (OC and EC). The 50% aerodynamic cutoff diameters of the impactors, $D_{50, \text{aero}}$, were 1.1 and 10 μm . The RH of the sampled air stream was measured a few inches upstream from the impactors. Throughout the paper submicrometer refers to particles with $D_{\text{aero}} < 1.1 \mu\text{m}$ at 60% RH and supermicrometer refers to particles with $1.1 \mu\text{m} < D_{\text{aero}} < 10 \mu\text{m}$ at 60% RH.

[10] Sub- and supermicrometer concentrations of Cl^- , NO_3^- , SO_4^{2-} , methanesulfonate (MSA^-), Na^+ , NH_4^+ , K^+ , Mg^{+2} , and Ca^{+2} were determined by ion chromatography (IC) [Quinn *et al.*, 1998]. Non-sea salt SO_4^{2-} , K^+ , Mg^{+2} , and Ca^{+2} concentrations were calculated by subtracting the sea-salt concentration (based on Na^+ concentrations and the ratio of the ion to sodium in seawater) from the total ion concentration. Sea salt aerosol concentrations were calculated as

$$\text{sea salt}(\mu\text{g m}^{-3}) = \text{Cl}^-(\mu\text{g m}^{-3}) + \text{Na}^+(\mu\text{g m}^{-3}) \times 1.47 \quad (1)$$

where 1.47 is the seawater ratio of $(\text{Na}^+ + \text{K}^+ + \text{Mg}^{+2} + \text{Ca}^{+2} + \text{SO}_4^{2-} + \text{HCO}_3^-) / \text{Na}^+$ [Holland, 1978]. This approach prevents the inclusion of non-sea salt K^+ , Mg^{+2} , Ca^{+2} , SO_4^{2-} , and HCO_3^- in the sea salt mass and allows for the loss of Cl^- mass through Cl^- depletion processes. It also assumes that all measured Na^+ and Cl^- is derived from seawater.

[11] Submicrometer and sub-10 μm samples were collected on pre-combusted quartz fiber filters using 2 and 1 stage impactors, respectively, for organic carbon (OC) and elemental carbon (EC) analysis [Bates *et al.*, 2004]. A charcoal diffusion denuder was deployed upstream of the submicrometer impactor to remove gas phase organic species. OC and EC concentrations were determined with a Sunset Laboratory thermal/optical analyzer. Three temperature

steps were used to evolve OC under O_2 -free conditions for quantification. The first step heated the filter to 230°C (the same temperature used in the thermodenuder as described below); the second step heated the filter to 600°C (AMS vaporizer temperature); and the final step heated the filter to 870°C. After cooling the sample down to 550°C, a He/O_2 mixture was introduced and the sample was heated in four temperature steps to 910°C to drive off EC. The transmission of light through the filter was measured to correct the observed EC for any OC that charred during the initial stages of heating. No correction was made for carbonate carbon so OC includes both organic and carbonate carbon. The percentage of carbonate carbon is unknown. OC samples were also collected with an impactor without a denuder. OC concentrations on these filters were three times higher than the denuded samples suggesting a significant positive artifact. The data from the non-denuded samples were not used in this manuscript.

[12] Submicron particles were collected on 37 mm Teflon filters for organic functional group analysis. After collection, the filters were frozen to prevent losses due to desorption or reaction, and transported back to San Diego for analysis by Fourier Transform Infrared (FTIR) spectroscopy. The FTIR spectra were analyzed using an automated algorithm that includes baselining, peakfitting, and integrating at specific peak locations to quantify organic functional group mass associated with major carbon bond types based on the method outlined by Maria *et al.* [2002] and revised by Russell *et al.* [2009]. Concentrations were calculated by dividing the mass of each functional group measured for each filter by the total volume of air sampled through the filter. Functional groups that were quantified include hydroxyl (including alcohol, COH), alkane (CCH), and amine (CNH₂). Carbonyl (C=O), carboxylic acid (COOH), aromatic, alkene (C=CH), organosulfate and organonitrate functional groups were below the detection limit for all filters discussed here.

[13] Concentrations of submicrometer NH_4^+ , SO_4^{2-} , NO_3^- , particulate organic matter (POM) and sea salt were measured with both a quadrupole aerosol mass spectrometer (Q-AMS) (Aerodyne Research Inc., Billerica, MA, USA) [Jayne *et al.*, 2000] and an Aerodyne high resolution time of flight aerosol mass spectrometer (HR-ToF-AMS) [DeCarlo *et al.*, 2006; Canagaratna *et al.*, 2007]. The sample stream passed through a submicrometer impactor at 60% RH before entering each AMS. The species measured by the AMS are referred to as non-refractory (NR) and are defined as all chemical components that vaporize at the vaporizer temperature of $\sim 600^\circ\text{C}$. This NR mass includes most organic carbon species and inorganic species such as ammonium nitrate and ammonium sulfate salts but generally does not include mineral dust, elemental carbon, or sea salt. However, with the high concentrations of sea salt in the Sea Sweep samples, Na^{35}Cl , Na^{37}Cl , and various halide clusters were detected by the Q-AMS and to a lesser extent by the HR-ToF-AMS. The ionization efficiency of the Q-AMS was calibrated every few days with dry monodisperse NH_4NO_3 particles using the procedure described by Jimenez *et al.* [2003]. The instrument operated on a 5 min cycle with the standard AMS aerodynamic lens. The data reported here use a collection efficiency for the Q-AMS of 0.8 based on comparison of sulfate concentrations with filter samples analyzed by ion chromatography during CalNEX. The HR-ToF-AMS was operated on a

2.5 min cycle, and data were acquired in the more sensitive V ion ToF mode, alternating between mass spectrum (MS) and particle time of flight (pToF) modes. The HR-ToF-AMS data were analyzed using the high resolution AMS data analysis software packages SQUIRREL 1.10 H and PIKA v1.10 H (D. Sueper, ToF-AMS Analysis Software, 2010, available at <http://cires.colorado.edu/jimenez-group/ToFAMSResources/ToFSoftware/index.html>). The data reported here assume a collection efficiency of 0.5 based on comparison to the Q-AMS. The aerodynamic particle beam forming lens on the front end of the AMS efficiently samples particles with aerodynamic diameters between 60 and 600 nm [Jayne *et al.*, 2000]. For ambient atmospheric samples, this size range generally captures the accumulation mode aerosol and thus is readily comparable to impactor samples of submicrometer aerosol. This is not the case for sea spray particles where the dominant mass mode tails into the submicrometer size range.

[14] Concentrations of black carbon were measured using a single particle soot photometer (SP2) (Droplet Measurement Technologies, Boulder, CO, USA) [Schwarz *et al.*, 2006]. The SP2 quantifies black carbon mass on a single particle basis by measuring the intensity of incandescent light produced after heating the particles to $>4000^{\circ}\text{C}$ using an intracavity laser at $1.064\ \mu\text{m}$. Black carbon mass concentrations are determined from the ensemble particle statistics. The SP2 detects particles with volume equivalent diameters between $\sim 60\text{--}650\ \text{nm}$ ($0.2\text{--}250\ \text{fg/particle}$). The SP2 was calibrated during CalNEX using atomized and size-selected “Regal black” particles [Moteki and Kondo, 2010].

2.4. Sea Sweep Aerosol Number Size Distributions

[15] One of the 21 mast tubes was used to supply air to a short column differential mobility particle sizer (Aitken-DMPS), a medium column differential mobility particle sizer (Accumulation-DMPS) and an aerodynamic particle sizer (APS, TSI model 3321). The two DMPSs were located in a humidity-controlled box (RH = 60%) at the base of the mast. The Aitken-DMPS was a short column University of Vienna [Winklmayr *et al.*, 1991] instrument connected to a TSI 3760A particle counter (TSI, St. Paul, MN) operating with a positive center rod voltage to sample particles with a negative charge. Data were collected in 10 size bins from 20 to 200 nm geometric diameter. The Aitken-DMPS operated with an aerosol flow rate of $1\ \text{L min}^{-1}$ and a sheath airflow rate of $10\ \text{L min}^{-1}$. The Accumulation-DMPS was a medium column University of Vienna instrument connected to a TSI 3760A particle counter operating with a positive center rod voltage to sample particles with a negative charge. The aerosol was charged with a Kr^{85} charge neutralizer (TSI model 3077) upstream of each DMA also at 60% RH. Data were collected in 7 size bins from 200 to 800 nm diameter. The Accumulation-DMPS operated with an aerosol flow rate of $0.5\ \text{L min}^{-1}$ and a sheath airflow rate of $5\ \text{L min}^{-1}$. The relative humidity of the sheath air for both DMPSs was controlled resulting in a measurement RH in the DMPSs of approximately 60%. With this RH control the aerosol should not have effloresced if it was hydrated in the atmosphere [Carrico *et al.*, 2003]. Mobility distributions were collected every 5 min.

[16] The mobility distributions were inverted to a number distribution assuming a Fuchs-Boltzmann charge

distribution from the charge neutralizer. The overlapping channels between the two instruments were eliminated in the inversion. The data were corrected for diffusional losses and size dependent counting efficiencies. The estimated uncertainty in the number concentration in each bin, based on flow uncertainties was $\pm 10\%$. The DMPS data were converted from geometric diameters to aerodynamic diameters using calculated densities and the water masses associated with the inorganic ions at the measurement RH. The densities and associated water masses were calculated with a thermodynamic equilibrium model (AeRho) using the measured chemical data [Quinn *et al.*, 2002].

[17] The APS was located in the lower humidity controlled box (60% RH) at the base of the mast. The inlet to the APS was vertical and its sample withdrawn isokinetically from the larger flow to the DMPS. The APS was modified to minimize internal heating of the sample flow in the APS by its sheath flow and waste heat and thus maintain 60% RH [Bates *et al.*, 2005]. Number size distributions were collected with the APS every 5 min. The APS data were collected in 34 size bins with aerodynamic diameters ranging from 0.96 to $10.37\ \mu\text{m}$. The estimated uncertainty in the supermicrometer size distribution was $\pm 10\%$.

2.5. Sea Sweep Aerosol Volatility

[18] One of the 21 mast tubes was used to supply air to a thermodenuder [Wehner *et al.*, 2002] twin Scanning Mobility Particle Sizer (SMPS) system. The $30\ \text{L min}^{-1}$ flow-passed through a submicrometer impactor at 60% RH and was then subsampled at $5\ \text{L min}^{-1}$ each into two $2.2\ \text{cm}$ ID tubes, one at ambient temperature and one heated to 230°C . The heated section was $0.61\ \text{m}$ long resulting in a residence time in the heated tube of $2.8\ \text{s}$. At the end of the heated tube, the flow-passed through a perforated stainless steel tube ($0.55\ \text{m}$) surrounded by a sheet of carbon-impregnated paper to remove the reactive gas phase species. The heated and unheated airflows were then isokinetically subsampled at the centerline at $2.0\ \text{L min}^{-1}$ and passed through nafion driers before entering the SMPSs (TSI 3080 coupled to a TSI 3010 CN counter). In addition to the twin SMPSs, the flows were sampled with TSI 3010 CN counters for a measure of the total particle number concentration heated and unheated. The twin systems were intercompared daily using an unheated flow and agreed in total number to within 10%. Tests with ammonium sulfate aerosol showed a complete removal of aerosol particle number in the thermodenuder.

2.6. Sea Sweep Aerosol Hygroscopic Growth

[19] One of the 21 mast tubes was used to supply air to a volatility-hygroscopicity tandem differential mobility analyzer (VH-TDMA) [Massoli *et al.*, 2010]. The $30\ \text{L min}^{-1}$ flow-passed through a submicrometer impactor at 60% RH and a sub-sampled part of that flow was first dried with a Nafion dryer (Perma Pure LLC, Toms River, NJ) and then with a silica gel diffusion dryer (Model DDU 570/H, Topas GmbH, Dresden, Germany) to ensure a RH less than 20%. The aerosol was neutralized with a radioactive aerosol neutralizer and a monodisperse aerosol was separated from a dried aerosol population with a DMA (Medium column Vienna type [Winklmayr *et al.*, 1991]). The monodisperse aerosol was sampled by two DMAs (Medium column Vienna

type [Winklmayr *et al.*, 1991]) operated in parallel. The sample was either passed directly to the second set of DMAs, or passed through a thermal denuder, using a 3-way solenoid valve. One of these DMAs measured the dry size and the second measured the size after the aerosol was humidified to the 90% RH. A full measurement cycle for a certain size with a certain denuder temperature and RH consisted of a size distribution scan with and without the thermal denuder. TSI 3010 and TSI 3772 particle counters were used to count the particles for dry and humidified size distributions respectively.

[20] The VH-TDMA was set to measure three particle sizes: 50 nm, 100 nm and 145 nm. The size distribution scan for each size took 240 s with the thermal denuder, and 180 s without. The thermal denuder was set to ramp the temperature up and down in a range from 50°C to 280°C in a 45 min interval.

[21] The growth factor spectrum was inverted according to Gysel *et al.* [2009]. The hygroscopicity side of the instrument was constructed following suggestions of Swietlicki *et al.* [2008]. Instrument calibration was regularly verified with generated ammonium sulphate at 90% RH. Dry size calibrations were conducted during every measurement cycle for all the dry sizes.

2.7. Sea Sweep Aerosol Cloud Condensation Nuclei Concentration

[22] A Droplet Measurement Technologies (DMT) CCN Counter [Roberts and Nenes, 2005; Lance *et al.*, 2006] was used to determine CCN concentrations of 60 nm particles at supersaturations, S , of 0.3, 0.4, 0.5, 0.6, and 0.7%. An SMPS was used to size-select 60 nm dry diameter particles that were sampled in parallel by the CCN counter and a TSI 3010 particle counter. Each supersaturation was sampled for 5 min. The first 2 or 3 min (depending on supersaturation) of each 5 min period were discarded so that only periods with stable supersaturations were included in the data analysis.

[23] The CCN counter was calibrated before and during the experiment as outlined by Lance *et al.* [2006]. An $(\text{NH}_4)_2\text{SO}_4$ aqueous solution was atomized with dry air, passed through a diffusional drier, diluted and then introduced to a SMPS (TSI). The resulting monodisperse aerosol stream was sampled simultaneously by the CCN counter and a water-based Condensation Particle Counter (WCPC, TSI) in order to determine the average activated fraction (CCN/CN). This procedure was repeated for a range of particle sizes and instrumental supersaturations. Using this procedure, the instrument supersaturation is equal to the critical supersaturation of the particle obtained from the activation curve for an activated fraction of 50%. The critical supersaturation for a given particle size was calculated from Kohler theory [e.g., Fitzgerald and Hoppel, 1984]. The supersaturations reported in the text are based on the calibrations and not the instrumental readout which disregards thermal efficiency. The difference between the calibrated values and those reported by the instrument were similar to the difference found by Lance *et al.* [2006]. The uncertainty associated with the CCN number concentrations is estimated to be less than $\pm 10\%$ [Roberts and Nenes, 2005]. Uncertainty in the instrumental supersaturation is less than $\pm 1\%$ for the operating conditions of this experiment [Roberts and Nenes, 2005].

2.8. Sea Sweep Aerosol Light Absorption and Extinction

[24] Light absorption by suspended sub-micrometer Sea Sweep particles was measured at 405 nm and 532 nm using the UC Davis (UCD) Photoacoustic Absorption Spectrometer (PAS) [Lack *et al.*, 2012] and light extinction was measured at 532 nm using the UCD Cavity Ring-Down Spectrometer (CRDS [Langridge *et al.*, 2011]). Measurements were made at a RH of 25% ($\pm 5\%$) following drying with a Nafion drier (Perma Pure). The detection limits for the 405 nm and 532 nm PAS channels during the Sea Sweep periods were around 0.3 Mm^{-1} and 0.1 Mm^{-1} , respectively, which correspond to a detection limit for black carbon [BC] of around 30 ng m^{-3} and 12 ng m^{-3} (assuming mass absorption coefficients for BC of $10 \text{ m}^2 \text{ g}^{-1}$ and $7.75 \text{ m}^2 \text{ g}^{-1}$ at 405 nm and 532 nm [Bond and Bergstrom, 2006; Cross *et al.*, 2010]). For extinction, the detection limits were 0.13 Mm^{-1} and 0.05 Mm^{-1} at 405 nm and 532 nm, respectively. Detection limits were determined as 3 times the standard deviation of the mean of the background measurements (i.e., air sampled through a filter) during the Sea Sweep periods. Measurements of absorption and extinction were made during Sea Sweep deployments 4, 6, 7 and 8.

2.9. Seawater Chlorophyll, Particulate Organic Carbon, and Dimethylsulfide

[25] Seawater entered the ship from the bow uncontaminated sampling line 5 m below the surface. Fluorescence (chlorophyll) was measured continuously with a Turner AU-10 Fluorometer equipped with a flow-through cell. The continuous-flow fluorometer was calibrated using discrete samples taken three times per day during both day and night. The discrete samples were filtered onto GF/F filters and frozen until analysis after the cruise. The filters were extracted with 90% acetone in a freezer for 24 to 30 h. The extract was analyzed on a Turner Designs 10-005 R fluorometer calibrated with commercial chlorophyll a.

[26] Seawater samples were collected from the uncontaminated sampling line (same as was used for the fluorescence measurements) during each Sea Sweep deployment. The samples were filtered through combusted quartz fiber filters and the filters were analyzed with the same Sunset Laboratory thermal/optical analyzer and temperature program used for the Sea Sweep aerosol samples (see section 2.3).

[27] Seawater samples were taken from the uncontaminated sampling line every 60 min for dimethylsulfide (DMS) analysis. The analysis consisted of a purge and trap collection followed by gas chromatography and quantification of DMS using a sulfur chemiluminescence detector [Bates *et al.*, 2008].

3. Results and Discussion

[28] Sea Sweep was deployed 11 times from the *R/V Atlantis* during CalNEX. Figure 2 indicates the locations of the deployments along the California coast. During the first two deployments, ambient air was not completely excluded from the Sea Sweep hood. They are therefore not included in this analysis. Subsequent to deployment 2, the area of the open ends was reduced to 1.0 cm to increase the face velocity of the curtain flow. The blank values of the hood with curtain

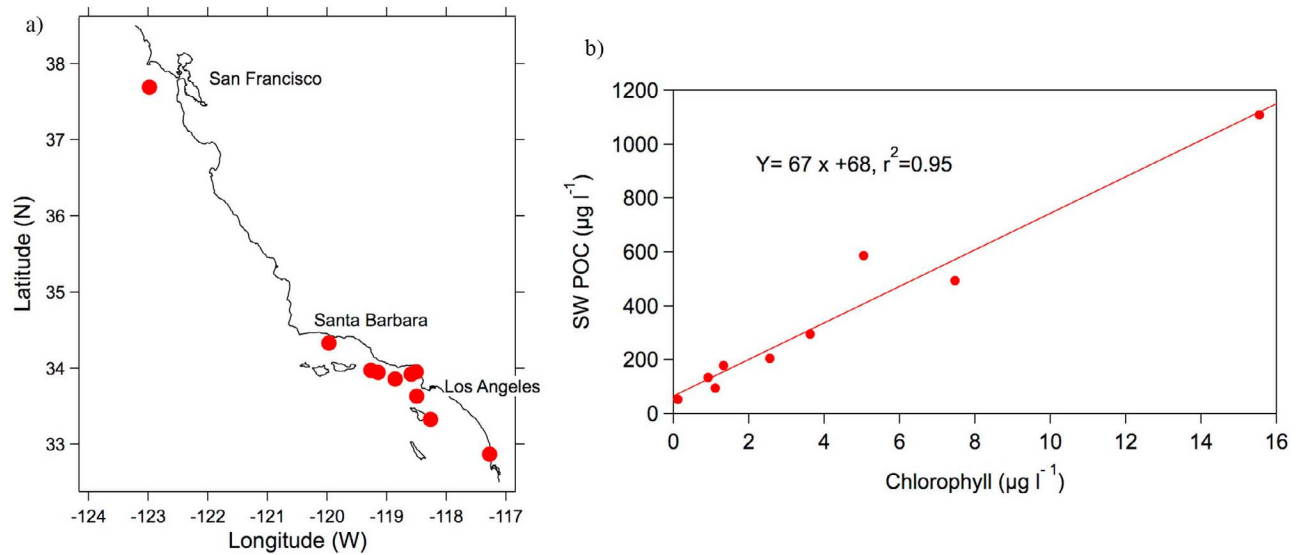


Figure 2. (a) Locations of Sea Sweep deployments during CalNEX (May 15–June 6, 2010). (b) Seawater chlorophyll ($\mu\text{g L}^{-1}$) and particulate organic carbon ($\mu\text{g C L}^{-1}$) at each Sea Sweep deployment. Seawater particulate organic carbon is operationally defined as that retained on a quartz fiber filter.

flow and no bubbler flow were checked before sampling at each deployment and whenever the sea state changed. The blank value was generally less than $20 \text{ particles cm}^{-3}$, and was not detectable in the number size distribution (Figure 3). The fifth deployment was aborted due to high winds that could not be effectively blocked in the lee of the ship and also is excluded from this analysis.

[29] Chlorophyll concentrations in the coastal surface waters during the Sea Sweep deployments ranged from <1 to $>15 \mu\text{g L}^{-1}$ (Figure 2). These concentrations are an order of magnitude higher than open-ocean North Atlantic chlorophyll concentrations [O'Dowd *et al.*, 2008]. Chlorophyll concentrations were highly correlated ($r = 0.98$) with seawater

particulate organic carbon (Figure 2) that ranged from 50 to $1100 \mu\text{g C L}^{-1}$. Particulate organic carbon is defined here as the OC retained on the quartz fiber filter during filtration. The filtrate is operationally defined as dissolved organic carbon (DOC) and comprised on average, 97% of the OC in seawater [Benner, 2002]. DOC exists in a continuum of sizes and includes macromolecular organic matter [Aluwihare *et al.*, 1997] and marine microcolloids [Benner *et al.*, 1992] that can be isolated from dissolved organic matter by ultrafiltration. The ultrafiltered dissolved organic matter has been reported to make up 23 to 33% of total dissolved organic carbon [McCarthy *et al.*, 1996] and is generally characterized by a large contribution of low molecular weight material

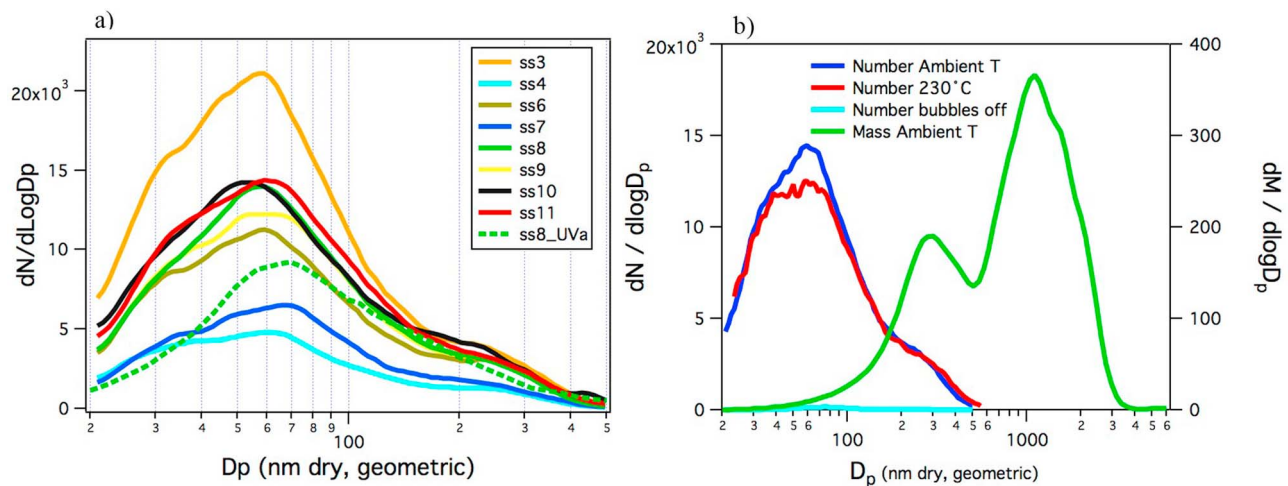


Figure 3. (a) Number size distributions from the ambient temperature SMPS averaged over each Sea Sweep deployment. The height of the mode was dependent on the number of bubbles caught in the Sea Sweep. The fine frit number size distribution from the University of Virginia (UVA) bubbler is shown for comparison. (b) The heated (230°C) and ambient temperature number size distributions for Sea Sweep deployment 11. Also shown is the mass size distribution from the DMPS/APS system. The sub-100 nm particles make up a very small fraction of the mass integrated over the entire size distribution.

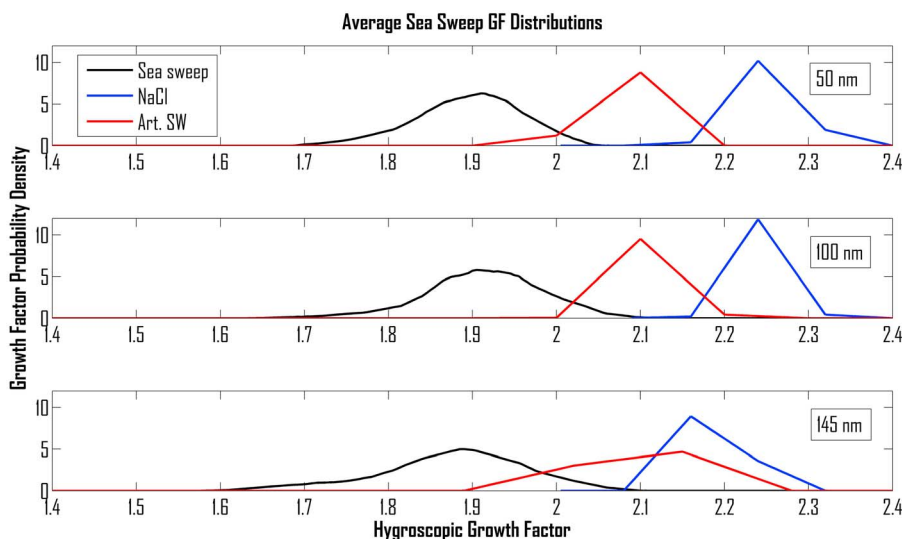


Figure 4. Average hygroscopic growth (dry to 90%RH) of selected particle sizes for Sea Sweep aerosol, NaCl, and artificial seawater particles. The data shown were not corrected for particle shape. Assuming a cubical shape would increase the growth factors by 1–3%.

(60–75% < 1 kDa) and a smaller contribution of high molecular weight material (>1 kDa) [Benner, 2002]. The concentration of the entire “dissolved” pool of organic carbon in the open ocean is within the range of 0.4 to 1 mg C L⁻¹ [Aluwihare *et al.*, 1997; Ogawa, 2000].

[30] The number size distribution of the directly emitted (nascent) Sea Sweep aerosol particles had a dominant mode at 55–60 nm (dry diameter) and secondary modes at 30–40 and 200–300 nm evident only as shoulders in the distribution (Figure 3). The absolute number concentration (integrated area under the curves shown in Figure 3) was dependent on the bubble airflow rate and the number of bubbles “captured” by the Sea Sweep. If the current was strong in the surface waters the generated bubbles would trail behind the Sea Sweep and not be efficiently captured by Sea Sweep hood assembly. The size distributions reported here are very similar to laboratory-generated particle size distributions using artificial and genuine seawater that show a dominant number mode in the 50–100 nm dry diameter size range [Mårtensson *et al.*, 2003; Keene *et al.*, 2007; Tyree *et al.*, 2007; Fuentes *et al.*, 2010; Hultin *et al.*, 2010]. The Sea Sweep distributions were also similar to measured number size distributions downwind of coastal breaking waves where Clarke *et al.* [2006] found a dominant number mode at 40 nm diameter and a secondary mode at 200 nm.

[31] During Sea Sweep deployments, a high-capacity particle generator (similar to that described by Keene *et al.* [2007]) was operated in parallel by the University of Virginia (UVA). The number size distributions produced by Sea Sweep were similar to those produced by the UVA generator (Figure 3) although the UVA distributions did not show the secondary mode at 30–40 nm. Fuentes *et al.* [2010] showed that the particle production method affects the shape of the particle size distribution. This could be further tested in future Sea Sweep deployments by using different frits.

[32] Heating the Sea Sweep sample stream to 230°C reduced the number of sub-100 nm particles by roughly 10% (Figure 3). The difference between the heated and unheated

size distributions was within the measurement uncertainties indicating that the bulk of the particles were not externally mixed sulfate or semi-volatile organics.

[33] The hygroscopic growth factors of the 50, 100, and 145 nm diameter particles at 90% RH in the Sea Sweep aerosol had a single homogeneous mode that was 10% smaller than artificial seawater generated in the laboratory (Figure 4). This suggests the presence of organic compounds internally mixed with sea salt. Fuentes *et al.* [2011] found a similar single mode with a 9–13% reduction in the growth factor when 2 mg C L⁻¹ of algal exudate was added to artificial seawater. Observations of aerosol hygroscopic growth in the remote Southern Hemisphere marine atmosphere during the ACE-1 Intensive Campaign [Berg *et al.*, 1998] revealed sea salt particles at 50 (number fraction = 0.16) and 150 nm (number fraction = 0.39) dry particle diameter with growth factors of 2.1. A growth factor of 2.1 suggests that these particles did not contain any appreciable organic content. ACE-1 took place in November/December when the surface waters were in transition from deeply mixed, winter conditions to the shallowly stratified, spring conditions [Griffiths *et al.*, 1999]. This resulted in low standing stocks of chlorophyll, tightly coupled phytoplankton growth and microzooplankton grazing rates, and low DMS concentrations [Griffiths *et al.*, 1999], conditions quite different from that measured during CalNEX. Clarke *et al.* [2006] measured hygroscopic growth factors of sea spray aerosols on the beach in Hawaii that were identical to that of seawater. The biological conditions during the study were not measured. Their studies included a flame photometric aerosol sodium detector that confirmed that particles down to 90 nm diameter contained Na. The apparently low organic enrichments in the samples collected by Clarke *et al.* [2006] relative to other studies [e.g., Keene *et al.*, 2007; Facchini *et al.*, 2008] also raises questions regarding the representativeness of aerosols produced by coastal breakers.

[34] Measurements of CCN concentrations confirmed that non-sea salt chemical species had only a limited impact on

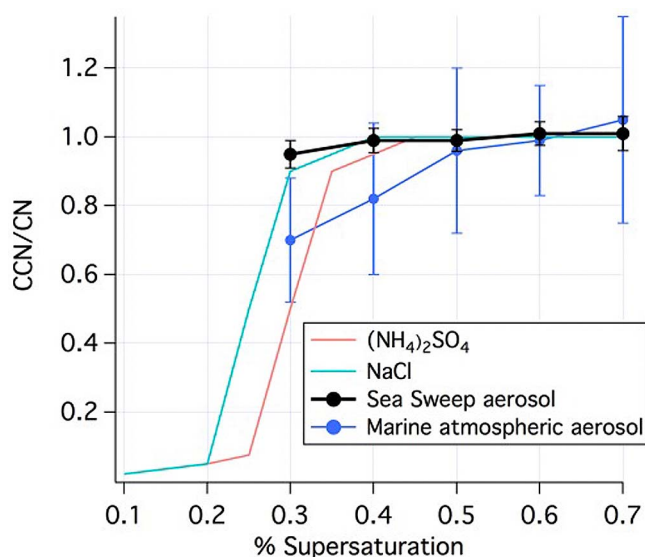


Figure 5. The CCN/CN ratio for 60 nm Sea Sweep aerosol particles as a function of supersaturation. Also shown is the CCN/CN ratio for 60 nm marine atmospheric aerosol particles sampled during a period of the CalNEX cruise that was minimally impacted by continental sources (total particle concentration = $90 \pm 8 \text{ cm}^{-3}$, submicrometer scattering = $2 \pm 0.3 \text{ Mm}^{-1}$, and submicrometer absorption below detection limit). Sixty nm $(\text{NH}_4)_2\text{SO}_4$ and NaCl particles are shown for comparison.

the hygroscopicity of the Sea Sweep aerosol for the range of supersaturations tested (0.3 to 0.7%). The CCN/CN activation ratio for 60 nm Sea Sweep particles was near 1 for all supersaturations indicating that all of the particles took up water and grew to cloud drop size. As shown in Figure 5, this behavior is similar to that of NaCl and indicates that the nascent ocean-derived particles were more hygroscopic than ammonium sulfate and atmospheric aerosol sampled in marine air masses (P. K. Quinn et al., manuscript in preparation, 2012).

[35] Chemical analysis of the dominant sub-100 nm mode is difficult since there is very little mass in this size range (Figure 3). The submicrometer sea salt mass concentrations from the impactor samples combined with the water mass associated with this sea salt at 60% RH could easily account for the mass [Quinn et al., 2002] derived from the DMPS-APS number size distributions (Figure 6). By mass, sea salt (dry) accounted for 93% of the total submicrometer mass (sum of the AMS-POM and impactor ion mass). The nascent aerosol was not enriched in SO_4 , Ca^{++} , K^+ , or Mg^{++} above that found in surface seawater. OC was <4% of the submicrometer mass (based on the Sunset Laboratory OC measurement). However, assuming a dissolved OC pool of 1 mg C L^{-1} [Aluwihare et al., 1997], the Sea Sweep aerosol was enriched in OC by a factor of 500 over the surface seawater concentration based on the OC/Na ratio in seawater and that measured in the Sea Sweep aerosol. OC in the Sea Sweep aerosol was not correlated with seawater chlorophyll or particulate organic carbon concentrations. This is consistent with the results of Facchini et al. [2008] who showed that organic matter in sea spray particles was more similar to the fine fraction (<10 μm diameter) than the bulk seawater

organic matter. Surface seawater chlorophyll concentrations during the Sea Sweep deployments varied by more than an order of magnitude while the submicrometer OC to sea salt ratio in the Sea Sweep samples remained relatively constant (0.036 ± 0.014). The bulk submicrometer impactor measurement made here does not allow for an assessment of the variability in the OC to sea salt ratio as a function of size. Higher size-resolution measurements of marine aerosol show that the carbon to sea salt ratio increases with decreasing particle diameter [Keene et al., 2007; Facchini et al., 2008].

[36] Submicrometer aerosol light absorption in the Sea Sweep sample air was near or below the limit of detection of the PAS (0.1 Mm^{-1} at 532 nm; 0.3 Mm^{-1} at 405 nm). The calculated black carbon (BC) concentrations from the PAS data (assuming a mass absorption coefficient of $7.75 \text{ m}^2 \text{ g}^{-1}$ at 532 nm and $10 \text{ m}^2 \text{ g}^{-1}$ at 405 nm) ranged from 7 to 35 ng m^{-3} . BC concentrations from the SP2 in this same sample air ranged from 3 to 44 ng m^{-3} . There was no correlation between BC and organic carbon or POM (AMS measurement of organic matter) suggesting different sources. The POM/BC ratio ranged from 28 to 230, which is higher than the POM/BC ratio (= 13) measured in the background atmosphere (defined by $\text{BC} < 20 \text{ ng m}^{-3}$) by Shank et al. [2011]. BC concentrations in the Sea Sweep sample air normalized to Na ranged from 0.001 to 0.006. BC/Na ratios in ambient air before/after the Sea Sweep deployments ranged from 0.12 to 3.3. There was no correlation between the BC/Na ratios in the Sea Sweep and ambient air samples. The BC in the Sea Sweep aerosol could be from combustion aerosol deposited on the ocean surface. While we cannot rule out contamination by ambient air as the source of these low BC concentrations in the Sea Sweep air, there was a step increase in the BC signal with the bubbler flow on versus the bubbler flow off.

[37] FTIR measurements suggest the submicrometer organic carbon mass composition was 53% hydroxyl, 33% alkane, and 14% amine. The high percentage of hydroxyl and alkane groups is similar to previous remote marine

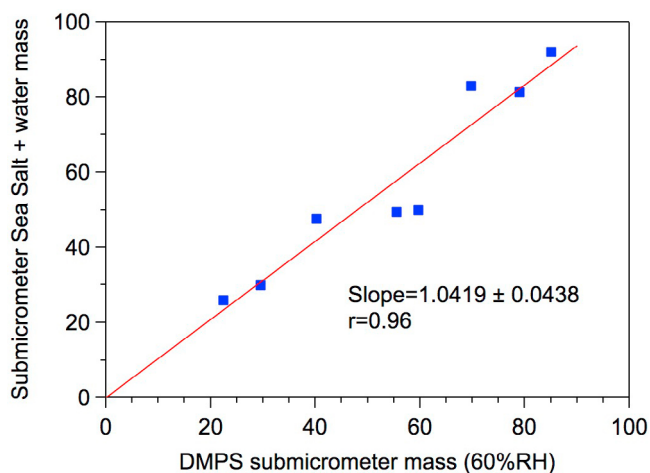


Figure 6. Sub-micrometer aerosol mass calculated from the aerosol number size distribution measured at 60% RH and mass of the chemically analyzed sea salt with the calculated water associated with sea salt at 60% RH (thermodynamic equilibrium model described in Quinn et al. [2002]).

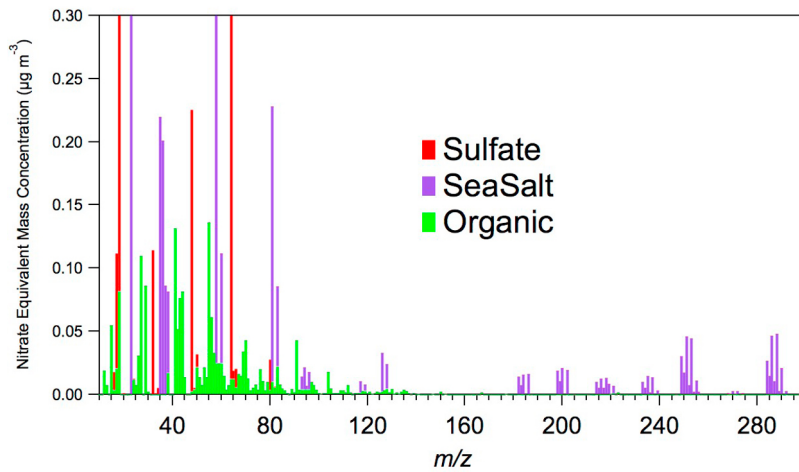


Figure 7. Q-AMS mass spectra of Sea Sweep deployment 11 off the coast of San Francisco.

atmospheric measurements [Russell *et al.*, 2010]. Lacking, however, were the carboxylic acid functional groups ubiquitously present in remote ocean atmospheric aerosol [Russell *et al.*, 2010]. This result suggests that these acid groups are predominantly a secondary product formed in the atmosphere.

[38] The Q-AMS mass spectrum of the Sea Sweep aerosol was dominated by halide clusters (Figure 7), evident from the ^{35}Cl and ^{37}Cl mass-to-charge (m/z) ratios. The HR-ToF-AMS confirmed the identification of these fragments and allowed for the assignment of each of these fragments to classes (Figure 8). The dominant organic non-oxygenated

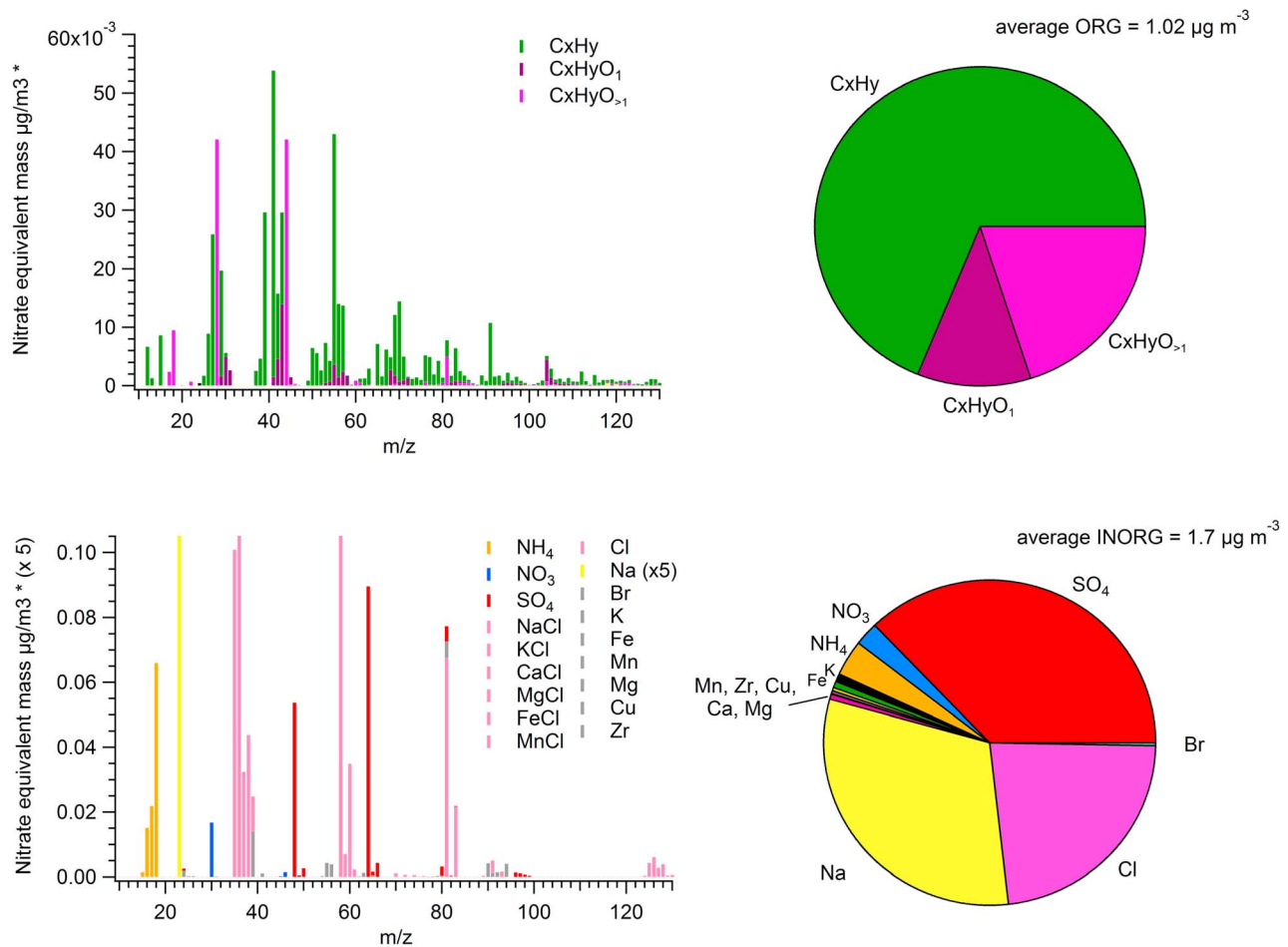


Figure 8. HR-ToF-AMS mass spectra and mass-weighted pie charts of the NR organic and inorganic components of Sea Sweep deployment 11.

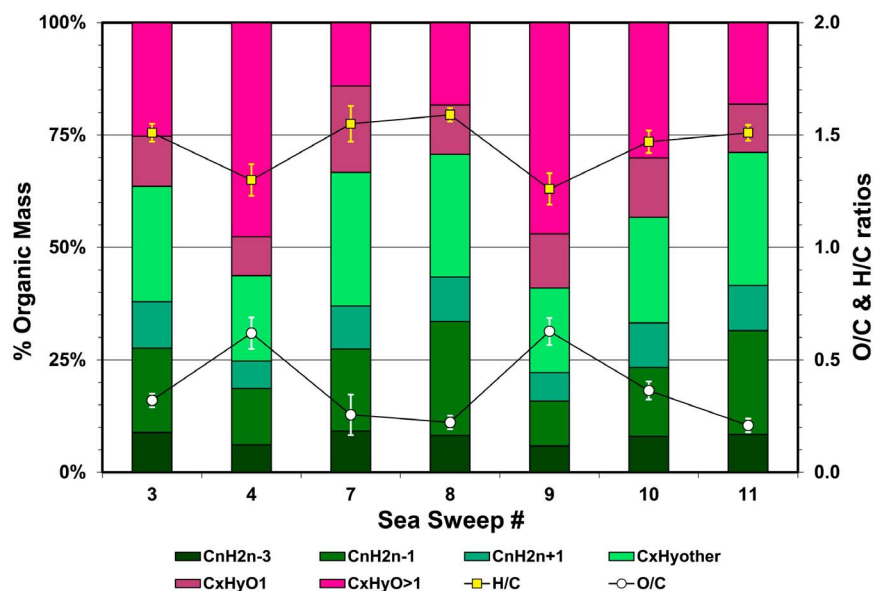


Figure 9. Organic mass fractions, O/C and H/C ratios in the Sea Sweep aerosol. Subcomponents of C_xH_yO are shown in green, while oxygenates are shown in pink colors.

hydrocarbon spectral fragments were m/z 27, 41, 55 (C_nH_{2n-1}: alkenes, cycloalkanes); m/z 29, 43, 57 (C_nH_{2n+1}: alkanes); and m/z 39, 53, 67 (C_nH_{2n-3}: dienes, alkynes, cycloalkenes). The dominant oxygenated spectral fragments included m/z 30, 31, 42 (C_xH_yO) and m/z 44, 45 (C_xH_yO_{>1}). Marker fragments for amino acids (m/z = 30, 42, 56) were also present but in very small amounts [Schneider *et al.*, 2011]. The organic aerosol was dominated by the non-oxygenated hydrocarbon classes (40–70%, average = 57.7%) of which approximately 50% was unsaturated hydrocarbons. Oxygenated hydrocarbons accounted for 28–58% (average = 40%) of the organic mass (Figure 9).

[39] The relative concentrations of inorganic and organic species detected by the HR-ToF-AMS are shown in Figure 8 for reference to other AMS measurements in the marine environment. The analysis assumes equal collection/ionization/vaporization efficiencies in the AMS for the inorganic and organic components. However, the SO₄/Na mass ratio in the AMS Sea Sweep sample was much greater than that of sea salt, likely due to the inefficient “flash” vaporization of NaCl at 600°C. The total inorganic mass is thus underestimated. The inefficient “flash” vaporization in the AMS also smears the time of flight data such that no clear mass size distributions were revealed for either the organic and inorganic components.

[40] The average POM/OC ratio from the AMS organic aerosol to Sunset Laboratory OC measurement was 1.9 ± 0.44 . The POM/OC ratio from the HR-ToF-MS was 1.6 ± 0.21 . While these ratios agree within the uncertainties of the measurements, the difference could also be attributed to a higher AMS organic collection efficiency than that used in these calculations. The average O/C and H/C molar ratios of the organic Sea Sweep aerosol were 0.37 ± 0.18 and 1.46 ± 0.13 , respectively, similar to that observed for average O/C and H/C molar ratios of marine plankton (0.35 and 1.67, respectively) [Whitehead, 2008]. The nascent Sea Sweep aerosol was less oxygenated (O/C = 0.37) than the marine

organic plume (O/C = 0.6) measured by *Ovadnevaite et al.* [2011a] at Mace Head, Ireland. Presumably the plume measured by *Ovadnevaite et al.* [2011a] would have been partially oxidized during transport.

[41] The concentration of POM present in the sea sweep aerosols as determined by the HR-ToF-MS ranged from $0.38\text{--}2.2 \mu\text{g m}^{-3}$. The sea salt normalized organic mass (both from the HR-ToF-MS) did not correlate with chlorophyll, but showed a statistically significant positive correlation with the concentration of DMS in the surface ocean ($R^2 = 0.51$, $n = 7$, Figure 10). As DMS is an indicator of oxidative stress and cell lysis in marine phytoplankton [Wolfe and Steinke, 1996], the correlation of organic aerosol with DMS suggests that the organic material in sea sweep aerosols observed here is related to phytoplankton cell lysis, most likely the cell exudate that would be highly concentrated in the sea surface microlayer.

[42] The alkene and C_xH_yO spectral fragments in the Sea Sweep aerosol are similar to those reported by *Ovadnevaite et al.* [2011a] downwind of a plankton bloom in the North Atlantic. The emission of marine aerosol with a large fraction of unsaturated organic hydrocarbons is also consistent with atmospheric measurements that have shown that primary submicrometer marine aerosol particles are dominated by insoluble organic colloids and aggregates [Facchini *et al.*, 2008; Rinaldi *et al.*, 2010]. Note that although these are dissolved organic carbon because of their size. In the surface ocean, dissolved organic carbon is photo-oxidized to formaldehyde, acetaldehyde and glyoxylate [Keiber *et al.*, 1990]. Glyoxylate in the surface ocean, being highly water soluble, cannot account for the glyoxal measured in the marine boundary layer [Sinreich *et al.*, 2010]. However, when dissolved organic carbon is emitted to the atmosphere as sea spray it plays a dual role as a source and sink for the OH radical leading to the production of low molecular weight organic compounds [Zhou *et al.*, 2008]. The unsaturated

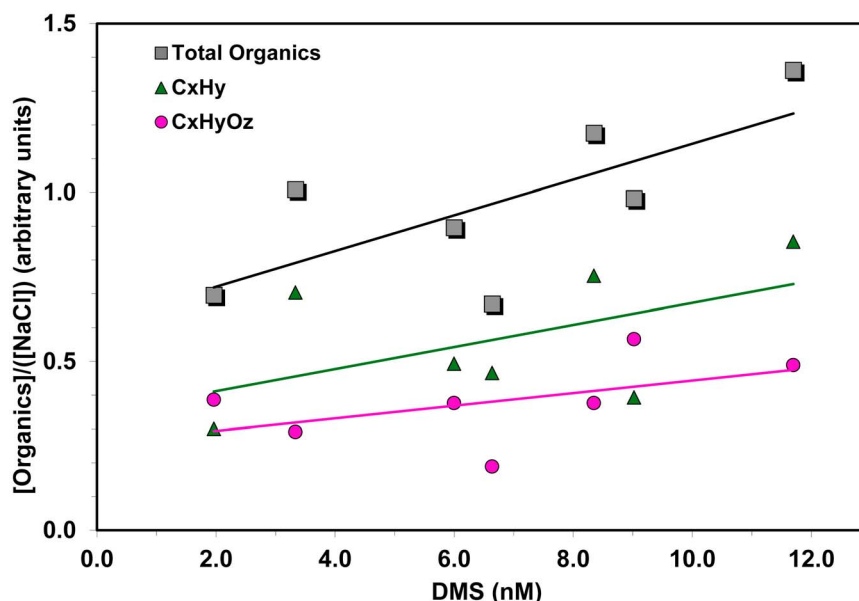


Figure 10. Correlation of surface seawater DMS concentrations with Sea Sweep aerosol organic concentrations normalized to Na^+Cl (organics and Na^+Cl from the HR-ToF-AMS). Total Organics: $y = 0.0529x + 0.6149$, $r^2 = 0.513$.

organic hydrocarbons in sea spray may be a likely source of atmospheric glyoxal through either OH or O_3 initiated oxidation.

4. Conclusions

[43] The Sea Sweep is an effective tool for in situ generation and sampling of nascent marine aerosol. By excluding ambient air with a curtain flow and varying the bubbler flow, the nascent particles can be diluted to a concentration that can be simultaneously sampled by a wide range of aerosol instrumentation.

[44] The first deployments off the coast of California showed a consistent aerosol number size distribution that closely resembled previous studies [Mårtensson *et al.*, 2003; Clarke *et al.*, 2006; Keene *et al.*, 2007; Tyree *et al.*, 2007; Fuentes *et al.*, 2010]. The aerosol was not volatile at 230°C and the dry submicrometer mass was largely sea salt ($>94\%$). The hygroscopic growth factor for 50, 100, and 145 nm diameter particles at 90% RH was 10% less than artificial seawater suggesting an internally mixed aerosol of sea salt with a small percentage of organic carbon. FTIR analysis suggested the organic mass was composed of carbohydrate-like compounds containing organic hydroxyl groups, alkanes and amines. Mass spectrometer analysis suggested the organic mass was highly unsaturated and minimally oxidized. Clearly, additional deployments will be needed to resolve these differences.

[45] The primary reason for studying the nascent marine aerosol is to better understand the source and composition of CCN over the ocean. While the submicrometer mass of the Sea Sweep particles is predominantly sea salt, the composition of the particles in the critical CCN size range (40–100 nm dry geometric diameter) is uncertain. Based on the hygroscopicity of the Sea Sweep aerosols the particles in this size range behave like sea salt with a small component of

organic matter. All 60 nm diameter particles were able to activate to cloud droplet size. In contrast, based on TEM analysis, Bigg and Leck [2008] show that in the regions of their measurements, particles in this size range are exopolymers produced by bacteria and algae and the microgels formed by them and do not include sea salt. In addition, direct measurements of the size-resolved chemical composition of marine aerosol that were produced from oligotrophic Sargasso Seawater [Keene *et al.*, 2007] and from more productive seawater in the eastern North Atlantic off Ireland [Facchini *et al.*, 2008] indicate that the dry mass of particles in this size range is dominated by organic constituents. These data are not necessarily contradictory if the organic carbon in this size range is composed of hygroscopic microgels [Bigg and Leck, 2008]. Ovadnevaite *et al.* [2011b] have shown that even when the atmospherically processed primary aerosols have a low hygroscopic growth factor, they can have a high CCN activity, presumably due to the enrichment of marine hydrogels in sea spray aerosol.

[46] Future Sea Sweep deployments must focus on resolving the chemical composition of the particles in the 40–200 nm diameter size range. Chemical sampling should target the smallest impactor stage ($D_{\text{aero}} < 0.18 \mu\text{m}$) as opposed to the $D_{\text{aero}} < 1.1 \mu\text{m}$ that was used during CalNEX. Hygroscopicity and CCN measurements should focus on particles at 30, 60, 200 nm diameter to investigate whether the three modes in the size distribution behave differently. TEM measurements of the Sea Sweep aerosol could also confirm the presence or absence of sea salt. Finally, measurements in the open ocean as opposed to the coastal measurements reported here would be more representative of the global sea spray flux to the atmosphere.

[47] **Acknowledgments.** This work was supported by the NOAA Atmospheric Composition and Climate Program. UHEL acknowledges additional financial support from the Academy of Finland Center of Excellence (1118615, 139656) and from the European Research Council

via project ATMNUCLE. York University acknowledges support from NSERC. UCD acknowledges additional financial support from the National Center for Environmental Research, EPA (RD834558). We thank Tim Smith, Dennis Holzer, and Christian Meinig for their assistance in the design and construction of Sea Sweep. We thank Derek Coffman, Drew Hamilton, James Johnson, Kristen Schulz, and Megan Haserodt for their assistance in sample collection and analysis as well as the captain and crew of the UNOLS R/V *Atlantis* for their support in the field. UHLE acknowledges Iyri Mikkilä and Mikael Ehn for their work developing the VHTDMA instrument and the data inversion routines. PMEL contribution 3818.

References

- Aluwihare, L. I., D. J. Repeta, and R. F. Chen (1997), A major biopolymeric component to dissolved organic carbon in surface sea water, *Nature*, **387**, 166–169, doi:10.1038/387166a0.
- Bates, T. S., D. J. Coffman, D. S. Covert, and P. K. Quinn (2002), Regional marine boundary layer aerosol size distributions in the Indian, Atlantic, and Pacific Oceans: A comparison of INDOEX measurements with ACE-1, ACE-2, and Aerosols99, *J. Geophys. Res.*, **107**(D18), 8026, doi:10.1029/2001JD001174.
- Bates, T. S., et al. (2004), Marine boundary layer dust and pollution transport associated with the passage of a frontal system over eastern Asia, *J. Geophys. Res.*, **109**, D19S19, doi:10.1029/2003JD004094.
- Bates, T. S., P. K. Quinn, D. J. Coffman, J. E. Johnson, and A. M. Middlebrook (2005), Dominance of organic aerosols in the marine boundary layer over the Gulf of Maine during NEAQS 2002 and their role in aerosol light scattering, *J. Geophys. Res.*, **110**, D18202, doi:10.1029/2005JD005797.
- Bates, T. S., et al. (2008), Boundary layer aerosol chemistry during TexAQS/GoMACCS 2006: Insights into aerosol sources and transformation processes, *J. Geophys. Res.*, **113**, D00F01, doi:10.1029/2008JD010023.
- Benner, R. (2002), Chemical composition and reactivity, in *Biogeochemistry of Marine Dissolved Organic Matter*, edited by D. A. Hansell and C. A. Carlson, pp. 59–90, Academic, Waltham, Mass., doi:10.1016/B978-012323841-2/50005-1.
- Benner, R., J. D. Pakulski, M. McCarthy, J. I. Hedges, and P. G. Hatcher (1992), Bulk chemical characterization of dissolved organic matter in the ocean, *Science*, **255**, 1561–1564, doi:10.1126/science.255.5051.1561.
- Berg, O. H., E. Swietlicki, and R. Krejci (1998), Hygroscopic growth of aerosol particles in the marine boundary layer over the Pacific and Southern Oceans during the first aerosol characterization experiment (ACE-1), *J. Geophys. Res.*, **103**(D13), 16,535–16,545, doi:10.1029/97JD02851.
- Berner, A., C. Lurzer, F. Pohl, O. Preining, and P. Wagner (1979), The size distribution of the urban aerosol in Vienna, *Sci. Total Environ.*, **13**, 245–261, doi:10.1016/0048-9697(79)90105-0.
- Bigg, E. K., and C. Leck (2008), The composition of fragments of bubbles bursting at the ocean surface, *J. Geophys. Res.*, **113**, D11209, doi:10.1029/2007JD009078.
- Bond, T. C., and R. W. Bergstrom (2006), Light absorption by carbonaceous particles: An investigative review, *Aerosol Sci. Technol.*, **40**, 27–67, doi:10.1080/02786820500421521.
- Canagaratna, M. R., et al. (2007), Chemical and microphysical characterization of ambient aerosols with the Aerodyne aerosol mass spectrometer, *Mass Spectrom. Rev.*, **26**, 185–222, doi:10.1002/mas.20115.
- Carrico, C. M., P. Kus, M. J. Rood, P. K. Quinn, and T. S. Bates (2003), Mixtures of pollution, dust, sea salt and volcanic aerosol during ACE-Asia: Light scattering properties as a function of relative humidity, *J. Geophys. Res.*, **108**(D23), 8650, doi:10.1029/2003JD003405.
- Cipriano, R. J., E. C. Monahan, P. A. Bowyer, and D. K. Woolf (1987), Marine condensation nucleus generation inferred from whitecap simulation tank results, *J. Geophys. Res.*, **92**, 6569–6576, doi:10.1029/JC092iC06p06569.
- Clarke, A. D., S. R. Owens, and J. Zhou (2006), An ultrafine sea-salt flux from breaking waves: Implications for cloud condensation nuclei in the remote marine atmosphere, *J. Geophys. Res.*, **111**, D06202, doi:10.1029/2005JD006565.
- Cross, E. S., et al. (2010), Soot particle studies—Instrument inter-comparison—Project overview, *Aerosol Sci. Technol.*, **44**, 592–611, doi:10.1080/02786826.2010.482113.
- DeCarlo, P. F., et al. (2006), Field-deployable, high-resolution, time-of-flight aerosol mass spectrometer, *Anal. Chem.*, **78**, 8281–8289, doi:10.1021/ac061249n.
- Facchini, M. C., et al. (2008), Primary submicron marine aerosol dominated by insoluble organic colloids and aggregates, *Geophys. Res. Lett.*, **35**, L17814, doi:10.1029/2008GL034210.
- Fitzgerald, J. W., and W. A. Hoppel (1984), Equilibrium size of atmospheric aerosol particles as a function of relative humidity: Calculations based on measured aerosol properties, in *Hygroscopic Aerosols*, edited by L. H. Ruhnke and A. Deepak, pp. 21–34, A. Deepak, Hampton, Va.
- Fuentes, E., H. Coe, D. Green, G. de Leeuw, and G. McFiggans (2010), Laboratory-generated primary marine aerosol via bubble-bursting and atomization, *Atmos. Meas. Technol.*, **3**, 141–162, doi:10.5194/amt-3-141-2010.
- Fuentes, E., H. Coe, D. Green, and G. McFiggans (2011), On the impacts of phytoplankton-derived organic matter on the properties of the primary marine aerosol—Part 2: Composition, hygroscopicity and cloud condensation activity, *Atmos. Chem. Phys.*, **11**, 2585–2602, doi:10.5194/acp-11-2585-2011.
- Griffiths, F. B., T. S. Bates, P. K. Quinn, L. A. Clementson, and J. S. Parslow (1999), Oceanographic context of the first aerosol characterization experiment (ACE 1): A physical, chemical, and biological overview, *J. Geophys. Res.*, **104**(D17), 21,649–21,671, doi:10.1029/1999JD900386.
- Gysel, M., G. B. McFiggans, and H. Coe (2009), Inversion of tandem differential mobility analyzer (TDMA) measurements, *J. Aerosol Sci.*, **40**, 134–151, doi:10.1016/j.jaerosci.2008.07.013.
- Holland, H. D. (1978), *The Chemistry of the Atmosphere and Oceans*, 154 pp., John Wiley, Hoboken, N. J.
- Hultin, K. A. H., E. D. Nilsson, R. Krejci, E. M. Mårtensson, K. Ehn, Å. Hagström, and G. de Leeuw (2010), In situ laboratory sea spray production during the MAP 2006 cruise on the North East Atlantic, *J. Geophys. Res.*, **115**, D06201, doi:10.1029/2009JD012522.
- Jayne, J. T., D. C. Leard, X. Zhang, P. Davidovits, K. A. Smith, C. E. Kolb, and D. R. Worsnop (2000), Development of an aerosol mass spectrometer for size and composition analysis of submicron particles, *Aerosol Sci. Technol.*, **33**, 49–70, doi:10.1080/027868200410840.
- Jimenez, J. L., et al. (2003), Ambient aerosol sampling using the Aerodyne Aerosol Mass Spectrometer, *J. Geophys. Res.*, **108**(D7), 8425, doi:10.1029/2001JD001213.
- Keene, W. C., et al. (2007), Chemical and physical characteristics of nascent aerosols produced by bursting bubbles at a model air-sea interface, *J. Geophys. Res.*, **112**, D21202, doi:10.1029/2007JD008464.
- Keiber, R. J., X. L. Zhou, and K. Mopper (1990), Formation of carbonyl compounds from UV-induced photodegradation of humic substances in natural waters: Fate of riverine carbon in the sea, *Limnol. Oceanogr.*, **35**, 1503–1515, doi:10.4319/lo.1990.35.7.1503.
- Lack, D. A., M. S. Richardson, D. Law, J. M. Langridge, C. D. Cappa, R. J. McLaughlin, and D. M. Murphy (2012), Aircraft instrument for comprehensive characterization of aerosol optical properties, part 2: Black and brown carbon absorption and absorption enhancement measured with photo acoustic spectroscopy, *Aerosol Sci. Technol.*, **46**, 555–568, doi:10.1080/02786826.2011.645955.
- Lance, S., J. Medina, J. N. Smith, and A. Nenes (2006), Mapping the operation of the DMT continuous flow CCN counter, *Aerosol Sci. Technol.*, **40**, 242–254, doi:10.1080/02786820500543290.
- Langridge, J. M., M. S. Richardson, D. Lack, D. Law, and D. M. Murphy (2011), Aircraft instrument for comprehensive characterization of aerosol optical properties, part 1: Wavelength-dependent optical extinction and its relative humidity dependence measured using cavity ringdown spectroscopy, *Aerosol Sci. Technol.*, **45**, 1305–1318, doi:10.1080/02786826.2011.592745.
- Leck, C., and E. K. Bigg (2005), Evolution of the marine aerosol—A new perspective, *Geophys. Res. Lett.*, **32**, L19803, doi:10.1029/2005GL023651.
- Maria, S. F., L. M. Russell, B. J. Turpin, and R. J. Porcja (2002), FTIR measurements of functional groups and organic mass in aerosol samples over the Caribbean, *Atmos. Environ.*, **36**(33), 5185–5196, doi:10.1016/S1352-2310(02)00654-4.
- Mårtensson, E. M., E. D. Nilsson, G. de Leeuw, L. H. Cohen, and H.-C. Hansson (2003), Laboratory simulations and parameterization of the primary marine aerosol production, *J. Geophys. Res.*, **108**(D9), 4297, doi:10.1029/2002JD002263.
- Massoli, P., et al. (2010), Relationship between aerosol oxidation level and hygroscopic properties of laboratory generated secondary organic aerosol (SOA) particles, *Geophys. Res. Lett.*, **37**, L24801, doi:10.1029/2010GL045258.
- McCarthy, M., J. Hedges and R. Benner (1996), Major biochemical composition of dissolved high molecular weight organic matter in seawater, *Mar. Chem.*, **55**, 281–297.
- Moteki, N., and Y. Kondo (2010), Dependence of laser-induced incandescence on physical properties of black carbon aerosols: Measurements and theoretical interpretation, *Aerosol Sci. Technol.*, **44**, 663–675, doi:10.1080/02786826.2010.484450.
- O'Dowd, C. D., and M. H. Smith (1993), Physicochemical properties of aerosols over the northeast Atlantic: Evidence for wind-speed-related

- sub-micron sea-salt aerosol production, *J. Geophys. Res.*, *98*(D1), 1137–1149, doi:10.1029/92JD02302.
- O'Dowd, C. D., B. Langmann, S. Varghese, C. Scannell, D. Ceburnis, and M. C. Facchini (2008), A combined organic-inorganic sea-spray source function, *Geophys. Res. Lett.*, *35*, L01801, doi:10.1029/2007GL030331.
- Ogawa, H. (2000), Bulk chemical aspects of dissolved organic matter in seawater review: The recent findings and unsolved problems, in *Dynamics and Characterization of Marine Organic Matter*, edited by N. Handa, E. Tanoie, and T. Hama, pp. 311–337, Terrapub, Tokyo.
- Ovadnevaite, J., C. O'Dowd, M. Dall'Osto, D. Ceburnis, D. R. Worsnop, and H. Berresheim (2011a), Detecting high contributions of primary organic matter to marine aerosol: A case study, *Geophys. Res. Lett.*, *38*, L02807, doi:10.1029/2010GL046083.
- Ovadnevaite, J., D. Ceburnis, G. Martucci, J. Bialek, C. Monahan, M. Rinaldi, M. C. Facchini, H. Berresheim, D. R. Worsnop, and C. O'Dowd (2011b), Primary marine organic aerosol: A dichotomy of low hygroscopicity and high CCN activity, *Geophys. Res. Lett.*, *38*, L21806, doi:10.1029/2011GL048869.
- Quinn, P. K., D. J. Coffman, V. N. Kapustin, T. S. Bates, and D. S. Covert (1998), Aerosol optical properties in the marine boundary layer during ACE 1 and the underlying chemical and physical aerosol properties, *J. Geophys. Res.*, *103*, 16,547–16,563, doi:10.1029/97JD02345.
- Quinn, P. K., D. J. Coffman, T. S. Bates, T. L. Miller, J. E. Johnson, E. J. Welton, C. Neusüss, M. Miller, and P. Sheridan (2002), Aerosol optical properties during INDOEX 1999: Means, variabilities, and controlling factors, *J. Geophys. Res.*, *107*(D19) 8020, doi:10.1029/2000JD000037.
- Rinaldi, M., S. Decesari, E. Finessi, L. Giulianelli, C. Carbone, S. Fuzzi, C. D. O'Dowd, D. Ceburnis, and M. C. Facchini (2010), Primary and secondary organic marine aerosol and oceanic biological activity: Recent results and new perspectives for future studies, *Adv. Meteorol.*, *2010*, 310682, doi:10.1155/2010/310682.
- Roberts, G. C., and A. Nenes (2005), A continuous-flow streamwise thermal gradient CCN chamber for atmospheric measurements, *Aerosol Sci. Technol.*, *39*, 206–221, doi:10.1080/027868290913988.
- Russell, L. M., S. Takahama, S. Liu, L. N. Hawkins, D. S. Covert, P. K. Quinn, and T. S. Bates (2009), Oxygenated fraction and mass of organic aerosol from direct emission and atmospheric processing measured on the R/V *Ronald Brown* during TEXAQS/GoMACCS 2006, *J. Geophys. Res.*, *114*, D00F05, doi:10.1029/2008JD011275.
- Russell, L. M., L. N. Hawkins, A. A. Frossard, P. K. Quinn, and T. S. Bates (2010), Carbohydrate-like composition of submicron atmospheric particles and their production from ocean bubble bursting, *Proc. Natl. Acad. Sci. U. S. A.*, *107*, 6652–6657, doi:10.1073/pnas.0908905107.
- Schneider, J., F. Freutel, S. R. Zorn, Q. Chen, D. K. Farmer, J. L. Jimenez, S. T. Martin, P. Artaxo, A. Wiedensohler, and S. Borrmann (2011), Mass-spectrometric identification of primary biological particle markers and application to pristine submicron aerosol measurements in Amazonia, *Atmos. Chem. Phys.*, *11*, 11,415–11,429.
- Schwarz, J. P., et al. (2006), Single-particle measurements of midlatitude black carbon and light-scattering aerosols from the boundary layer to the lower stratosphere, *J. Geophys. Res.*, *111*, D16207, doi:10.1029/2006JD007076.
- Shank, L. M., et al. (2011), Organic carbon and non-refractory aerosol over the remote southeast Pacific: Oceanic and combustion sources, *Atmos. Chem. Phys. Discuss.*, *11*, 16,895–16,932, doi:10.5194/acpd-11-16895-2011.
- Sinreich, R., S. Coburn, B. Dix, and R. Volkamer (2010), Ship-based detection of glyoxal over the remote tropical Pacific Ocean, *Atmos. Chem. Phys.*, *10*, 11,359–11,371, doi:10.5194/acp-10-11359-2010.
- Swietlicki, E., et al. (2008), Hygroscopic properties of sub-micrometer atmospheric aerosol particles measured with H-TDMA instruments in various environments—A review, *Tellus, Ser. B*, *60*, 432–469, doi:10.1111/j.1600-0889.2008.00350.x.
- Tyree, C. A., V. M. Hellion, O. A. Alexandrova, and J. O. Allen (2007), Foam droplets generated from natural and artificial seawaters, *J. Geophys. Res.*, *112*, D12204, doi:10.1029/2006JD007729.
- Wehner, B., S. Philippin, and A. Wiedensohler (2002), Design and calibration of a thermodenuder with an improved heating unit to measure the size-dependent volatile fraction of aerosol particles, *J. Aerosol Sci.*, *33*(7), 1087–1093, doi:10.1016/S0021-8502(02)00056-3.
- Whitehead, K. (2008), Marine organic geochemistry, in *Chemical Oceanography and the Marine Carbon Cycle*, edited by S. R. Emerson and J. I. Hedges, pp. 261–294, Cambridge Univ. Press, New York.
- Winklmayr, W., G. P. Reischl, A. O. Lindner, and A. Berner (1991), New electromobility spectrometer for the measurement of aerosol size distributions in the size range 1 to 1000 nm, *J. Aerosol Sci.*, *22*, 289–296, doi:10.1016/S0021-8502(05)80007-2.
- Wolfe, G. V., and M. Steinke (1996), Grazing-activated production of dimethyl sulfide (DMS) by two clones of *Emiliania huxleyi*, *Limnol. Oceanogr.*, *41*(6), 1151–1160, doi:10.4319/lo.1996.41.6.1151.
- Zhou, X., A. J. Davis, D. J. Kieber, W. C. Keene, J. R. Maben, H. Maring, E. E. Dahl, M. A. Izaguirre, R. Sander, and L. Smoydzyn (2008), Photochemical production of hydroxyl radical and hydroperoxides in water extracts of nascent marine aerosols produced by bursting bubbles from Sargasso seawater, *Geophys. Res. Lett.*, *35*, L20803, doi:10.1029/2008GL035418.